Evaluation of adsorption ability of Cyclodextrin-Calixarene Nanosponges towards Pb^{2+} ion in aqueous solution

Salvatore Cataldo[a], *Paolo Lo Meo*[b]*, *Pellegrino Conte*[c], *Antonella Di Vincenzo*[b], *Demetrio Milea*[d], *Alberto Pettignano*[a]*

[a] *Dipartimento di Fisica e Chimica - Emilio Segrè, Università di Palermo – V.le delle Scienze ed. 17, 90128 Palermo (Italy)*
[b] *Dipartimento di Scienze e Tecnologie Biologiche, Chimiche e Farmaceutiche (STEBICEF), Università di Palermo – V.le delle Scienze, ed. 17, 90128 Palermo (Italy)*
[c] *Dipartimento di Scienze Agrarie, Alimentari e Forestali (SAAF), Università di Palermo – V.le delle Scienze, ed. 4, 90128 Palermo (Italy)*
[d] *Dipartimento di Scienze Chimiche, Biologiche, Farmaceutiche ed Ambientali, Universita degli Studi di Messina, Viale F. Stagno d'Alcontres 31, 98166 Messina (Italy)*

***Corresponding Authors**
tel. (+39) 091 23897537; tel. (+39) 091 23897959
E-mail: paolo.lomeo@unipa.it ; alberto.pettignano@unipa.it

Highlights

- Some cyclodextrin-calixarene nanosponges were tested as sorbents for Pb^{2+} ion species.
- The materials can simultaneously sequestrate both inorganic and organic pollutants.
- Functionalization of the materials has a critical outcome on their sorbent abilities.
- Their abilities were rationalized in terms of functional mobility of the solvent medium.

ABSTRACT. In this study, different pristine and chemically post-modified cyclodextrin-calixarene nanosponges (CyCaNSs) have been characterized by means of FFC-NMR relaxometric techniques, and used as adsorbent materials to remove Pb^{2+} from aqueous solutions. Considering that the removal treatments may involve polluted waters with different characteristics, the adsorption experiments were performed on solutions without and with the addition of background salts, under different operational conditions. In particular, $NaNO_3$ and NaCl were used as salts to change the ionic strength in the range 0.01 ~ 0.1 mol L^{-1}; the initial pH of the treated solutions was

fixed at the values of either 3.0 or 5.0, while the effect of temperature was studied in the range 283.15~323.15 K. The adsorption abilities and affinities of the nanosponges towards Pb^{2+} were kinetically and thermodynamically investigated by measuring the metal ion concentration in the water samples of batch experiments by means of Inductively Coupled Plasma Emission Spectroscopy (ICP-OES) and Differential Pulse Anodic Stripping Voltammetry (DP-ASV). The acid-base properties of nanosponges and of metal ion as well as their interactions with the other interacting components of the systems have been considered in the evaluation of adsorption mechanism. Recycling and reuse experiments on the most efficient adsorbents were also performed. On the grounds of the results obtained, post-modified CyCaNSs appear promising materials for designing environmental remediation devices.

Keywords: Adsorption, FFC-NMR relaxometry, Lead, Nanosponges, Remediation, Speciation.

1. Introduction

Sorbent materials able to sequestrate at the same time both inorganic and organic species constitute valuable tools for designing environmental remediation devices, aimed at the treatment of polluted soils and waters, and in particular at the detoxification of wastewaters. Systems based on chitosan (Sarode et al., 2019; Zhu & Zhou, 2018), alginate (Cataldo, Cavallaro, et al., 2013; Cataldo, Gianguzza, Pettignano, & Villaescusa, 2013), graphene (Siyal, Shamsuddin, Low, & Rabat, 2020; Zhang, Hou, Huang, & Fan, 2020), biochars (Cataldo, Chiodo, et al., 2018; M. A. Rao, Di Rauso Simeone, Scelza, & Conte, 2017; Ravindiran, Ganapathy, Josephraj, & Alagumalai, 2019; Wang & Wang, 2019), yeasts (Massoud, Hadiani, Hamzehlou, & Khosravi-Darani, 2019; Qin, Hu, Zhai, Lu, & Aliyeva, 2020), etc. have been widely tested for these

purposes. In particular, an increasing attention has been recently paid to composite materials based on cyclodextrins (CDs) (Julinová & Slavík, 2012; Karoyo & Wilson, 2015; Tong & Yuan, 2012). In fact, these cyclic oligosaccharides gather several interesting and useful features (Szejtli, 1998). They can be considered as a sustainable material (being obtained via bacterial digestion of starch, and thereby constituting a renewable source). Moreover, they are highly functionalized molecules, containing plenty of primary and secondary hydroxyl groups liable to undergo chemical transformation by quite simple organic reaction routes (Khan, 1998). Furthermore, CDs are probably the most accessible and studied class of supramolecular hosts, able to form inclusion complexes with a large variety of diversely structured organic guest species (Rekharsky & Inoue, 1998). They can also interact with inorganic cations (Bonomo, Pedotti, Vecchio, & Rizzarelli, 1996; Bose & Polavarapu, 1999; Oliveri, Pietropaolo, Sgarlata, & Vecchio, 2017; Rizzarelli & Vecchio, 1999; Tabushi, Kuroda, & Mizutani, 1984; Yoshihisa, Toyoaki, & Yoshio, 1972) via their hydroxyl groups and any other suitable donor groups that could have been inserted by chemical modification, and can even stabilize metal nanoparticles (J. Liu et al., 1999; J. Liu, Ong, Kaifer, & Peinador, 2002; J. Liu, Ong, Román, Lynn, & Kaifer, 2000; M. Russo et al., 2015). The reaction between native or chemically modified CDs with suitable reticulating agents allows accessing to a further class of potential sorbent materials referred to as “Nanosponges” (NSs) (Caldera, Tannous, Cavalli, Zanetti, & Trotta, 2017; *Nanosponges: Synthesis and Applications*, 2019; Francesco Trotta, 2011; F. Trotta, Shende, & Biasizzo, 2012). Notwithstanding their insoluble hyper-cross-linked structure, NSs show an excellent permeability to aqueous media and a fair swellability (Paolo Lo Meo, Mundo, Terranova, Conte, & Chillura Martino, 2020), maintaining at the same time the inclusion abilities of the parent CDs. Therefore, NSs are excellent platforms to support nanosized catalysts (Noël et

al., 2014; Marco Russo et al., 2019; Vasconcelos et al., 2016) or to provide smart/tailored materials for controlled drug delivery (Allahyari, Trotta, Valizadeh, Jelvehgari, & Zakeri-Milani, 2019; Cavalli, Trotta, & Tumiatti, 2006; Chilajwar, Pednekar, Jadhav, Gupta, & Kadam, 2014; Swaminathan, Vavia, Trotta, & Torne, 2007; Francesco Trotta, Dianzani, Caldera, Mognetti, & Cavalli, 2014; Francesco Trotta, Zanetti, & Cavalli, 2012). Moreover, NSs are also ideal candidates as sorbent materials for environmental applications. The sequestration of metal cations, and the simultaneous adsorption of both inorganic and organic species by NS-based materials as well, has been occasionally explored (Morin-Crini & Crini, 2013; Sikder et al., 2019). For instance, promising results have been obtained in the simultaneous sequestration of Pb^{2+} ions and a dye (Acid Red), using a composite material based on βCD and chitosan cross-linked with glutaraldehyde and EDTA dianhydride (Wu et al., 2018). The simultaneous sequestration of Pb^{2+} ions and Bisphenol A or Methylene Blue with a material obtained reticulating the βCD with hexachloro-cyclotriphosphazene has been reported (Yinli Liu et al., 2019).

We have been recently interested in the synthesis and adsorption/release abilities of a new class of NSs obtained by co-polymerization of cyclodextrin and calixarene derivatives, which are joined together by means of 1,2,3-triazole linker units (Fontana et al., 2019; P. Lo Meo, Lazzara, Liotta, Riela, & Noto, 2014; Massaro et al., 2016). These materials (indicated hereinafter as CyCaNSs) benefit from the presence of two different co-monomers, having somehow complementary supramolecular host abilities, and from their viable chemical post-modification as well, which easily enables the introduction on the polymeric network of further functionalities such as amine or carboxyl groups (Cinà, Russo, Lazzara, Chillura Martino, & Lo Meo, 2017). Due to the presence of the aforementioned ionizable groups, these materials present pH-sensitive

adsorption/release abilities towards various probe guests such as *p*-nitroaniline derivatives, dyes and bioactive molecules (Di Vincenzo et al., 2019). Their acid-base properties have been recently assessed. Interestingly, it has been positively shown that the insertion in the polymeric network largely enhances (up to several order of magnitude) the basic strength of the triazole linker units (Di Vincenzo et al., 2019). In view of a possible utilization of CyCaNSs as materials for environment remediation purposes, an investigation of their possible sequestration abilities towards metal cations was needed. In particular, we paid attention to the Pb^{2+} ion for several reasons. Among toxic metal ions, indeed, lead is one of the most extensively used in several fields like, e.g., PVC production, ammunition, paints, vehicle batteries, etc. Moreover, lead is considered one of the most toxic metal. Exposure of plants, animals and humans to lead causes well known negative effects (Crompton, 2007). In particular, the long term exposure of humans can cause learning and behavioral difficulties in children, damage to liver and kidneys, reduction of bone growth and disease to immune system (Gidlow, 2015; Mason, Harp, & Han, 2014).

In the present study we investigated the adsorption abilities towards the Pb^{2+} ion of four selected CyCaNSs NS1-NS4 (Figure 1). More in detail, materials NS1 and NS2 are obtained by reacting, under the typical conditions of the well-known *CuAAC* coupling reaction (Meldal & Tornøe, 2008), the heptakis-(6-azido)-(6-deoxy)-βCD (**ACD**) and the tetrakis-propargyloxy-calix[4]arene (**PCA**) in two different equivalent ratios (2:1 and 1:2) respectively. These ratios were chosen in such a way that the resulting products possess either azide or alkyne unreacted functional groups, able to undergo further transformation (Cinà et al., 2017). Hence, material NS3 is obtained from NS1 by Staudinger reduction, whereas NS4 is obtained from NS2 by *CuAAC* reaction with ethyl azidoacetate and subsequent alkaline hydrolysis. All these materials have already undergone full structural and morphological characterization (FT-IR, $^{13}C[^{1}H]$ CP-

MAS SS-NMR, SEM, BET/BJH porosimetry) (Cinà et al., 2017; P. Lo Meo et al., 2014). Their average compositions are summarized in Table 1. Moreover, they have been tested for their pH-dependent adsorption abilities towards a set of diverse model pollutants, such as *p*-nitroaniline derivatives and commercial dyes (Bromocresol green, Toluidine blue, Methylorange), suitably selected according to their different size, shape, hydrophobic/hydrophilic character and possible presence of charged or ionizable groups.

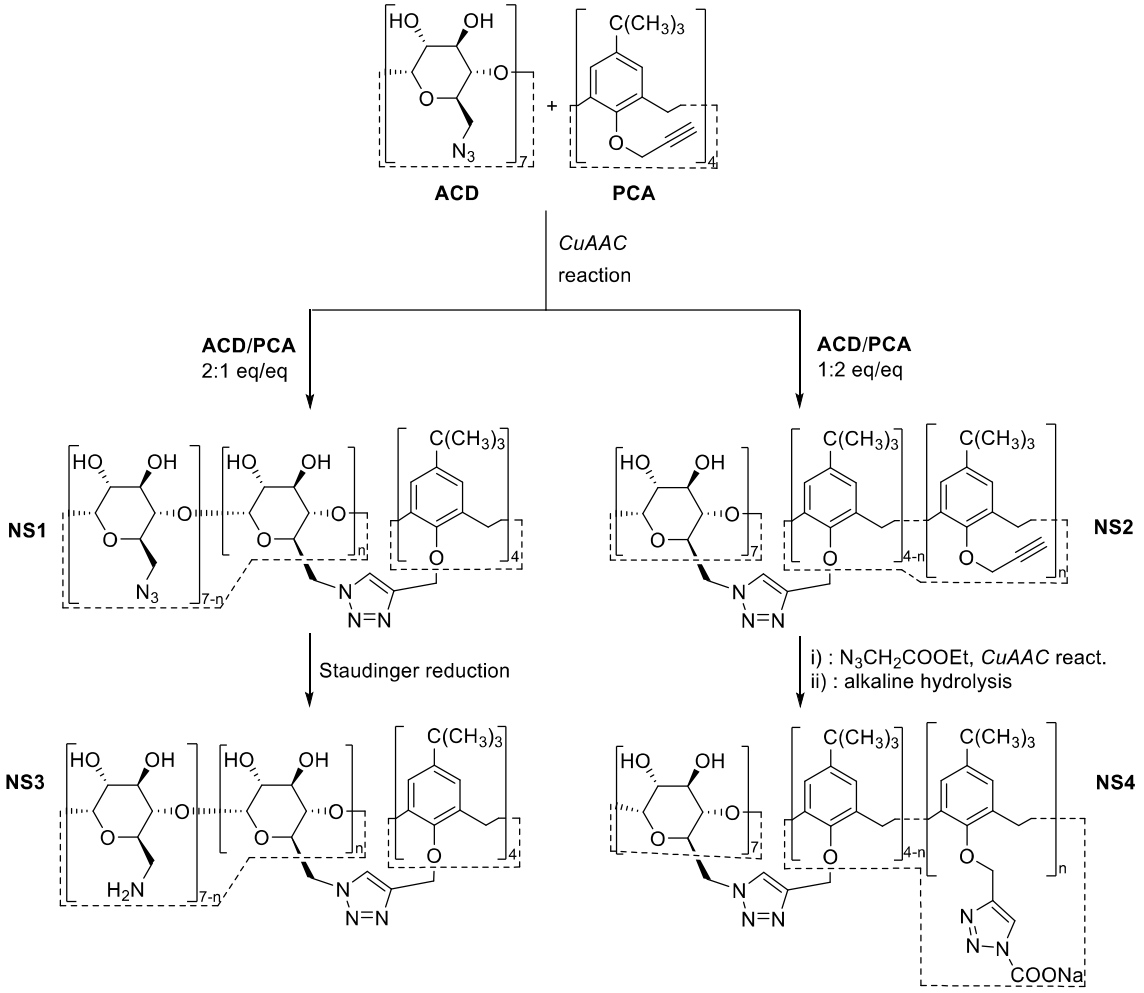

Figure 1. Nanosponges NS1-NS4.

Table 1. Average composition (mmol g^{-1}) of CyCaNSs.[a]

	co-monomers		from NMR			from potentiometric titration		
	PCA	ACD	Triazole groups	Amine groups	Carboxyl groups	Triazole groups	Amine groups	Carboxyl groups
NS1	0.495	0.461	1.66	-	-	0.49	-	-
NS2	0.847	0.246	1.46	-	-	0.42	-	-
NS3	0.518	0.481	1.66	1.71	-	0.40	0.68	-
NS4	0.677	0.196	2.71	-	1.64	0.69	-	0.75

[a] from ref. (Di Vincenzo et al., 2019).

2. Materials and Methods

2.1. Materials

The CyCaNSs NS1-NS4 had been already prepared for previous works (Cinà et al., 2017; Di Vincenzo et al., 2019). Sodium nitrate and sodium chloride pure salts (Fluka) were used, after drying at 383.15 K for 2 h, to adjust the ionic strength of solutions. Nitric acid, hydrochloric acid and sodium hydroxide used to adjust the pH of the metal ion solutions were prepared by diluting concentrated Fluka solutions. Pb^{2+} ion solutions were prepared by weighing the $Pb(NO_3)_2$ (Aldrich, analytical grade) salt. Standard solutions of the metal ion used for calibration curves were prepared by diluting 1000 mg L^{-1} standard solution in 2% HNO_3 (CertiPUR, Merck). All the solutions were prepared using freshly, CO_2-free ultrapure water ($\rho \geq 18$ MΩ cm) and grade A glassware.

2.2. Procedures for kinetic, thermodynamic and recycling experiments

Preliminary adsorption tests towards Pb^{2+} ion on the four CyCaNSs were performed by placing ca. 8 mg of each adsorbent material in an Erlenmeyer flask containing 20 mL of $Pb(NO_3)_2$,

152 solution (c_{Pb2+} = 42.3 mg L^{-1}), at pH = 5.0, in $NaNO_3$ 0.1 mol L^{-1} and at T = 298.15 K. The
153 solutions were stirred at 180 rpm for 24 hours using an orbital mixer (model M201-OR, MPM
154 Instruments) before measuring the metal ion concentration by means of DP-ASV technique.
155 Batch kinetic and thermodynamic adsorption experiments were carried out only with NS3 and
156 NS4 materials.
157 The kinetic experiments were carried out in $NaNO_3$, at I = 0.10 mol L^{-1} and T = 295.15 K. The
158 initial pH of the solution was adjusted at 5 and was monitored during the experiments. The
159 adsorbent material (15.0 mg) of was added to the solution containing the metal ion ($c_{Pb2+} \approx$ 35 mg
160 L^{-1}, 20 mL) in a voltammetric cell under constant and regular stirring. The metal ion
161 concentration in solution was measured at various adsorbent/solution contact times in the interval
162 0~400 minutes.
163 The voltammetric apparatus was constituted by a Metrohm 663 VA stand combined with the
164 Autolab potentiostat in conjunction with the IME663 interface. The voltammetric apparatus was
165 controlled by NOVA v. 1.10 software. The VA stand was equipped with a three electrode system
166 consisting of: *i*) a MultiMode Electrode Pro (Metrohm, code 6.1246.120) working in the Static
167 Mercury Drop Electrode (SMDE) mode; *ii*) a glassy carbon auxiliary electrode (code
168 6.1247.000); *iii*) a double junction Ag/AgCl/ KCl (3 mol·L^{-1}) reference electrode (code
169 6.0728.030). The DP-ASV measurements were performed after bubbling purified N_2 gas into the
170 solutions for 150 s. The experimental electrochemical conditions were chosen in order to
171 optimize the quality parameters, as signal/noise ratio, repeatability and accuracy (deposition
172 potential -0.55 V; deposition time 1 s; equilibration time 10 s; potential interval -0.55 to -0.20 V;
173 scan rate 0.01 V s^{-1}; step potential 3 mV; modulation amplitude 50 mV; modulation time 0.01 s;
174 interval time 0.2 s).

Isotherm experiments were carried out at pH 3 and 5, without ionic medium, in $NaNO_3$ 0.1 mol L^{-1} and in NaCl 0.01, 0.05 and 0.1 mol L^{-1}, in the temperature range 283.15 – 323.15 K. In each isotherm experiment, nine samples of either NS3 or NS4 (ca. 5 mg each) were placed in different Erlenmeyer flasks containing 10~15 mL of a $Pb(NO_3)_2$ solution ($5 \leq c_{Pb2+}$ / mg $L^{-1} \leq 70$). The solutions were stirred at 180 rpm for 12 hours using an orbital mixer (model M201-OR, MPM Instruments) and then were separated from the adsorbent before measuring the pH and the metal ion concentration.

The reuse and recycling of NS3 and NS4 were studied packing ~10 mg of each nanosponge into a glass column (diameter = 2 cm, length = 5 cm). 20 mL of $Pb(NO_3)_2$ solution (c_{Pb2+} = 35 mg L^{-1}, pH = 5.0, T = 298.15 K) were flowed at reflux into the column with a flow rate of 6 mL min^{-1} for 12 h (the reaching of adsorption equilibrium was verified) by using a peristaltic pump (Gilson, Minipuls 3). The sorbent material was then washed with 100 mL of distilled water before the Pb^{2+} desorption carried out with 20 mL of HNO_3 0.1 mol L^{-1} solution for 6 h. After a further washing with 100 mL of distilled water, the next test cycle began. The water samples derived from each adsorption and desorption step were collected in 50 mL test tubes. Four adsorption / desorption cycles were carried out for each adsorbent.

The Pb^{2+} concentration in the solutions collected in isotherm and recycling experiments was measured by Inductively Coupled Plasma Emission Spectroscopy (ICP-OES) technique by using a PerkinElmer Model Optima 2100, equipped with an auto sampler model AS-90. The Pb^{2+} emission intensities were measured at two wavelengths (194.168 and 253.652 nm) and each measurement was repeated three times. Calibration curves were done in the same experimental conditions and covering the metal ion concentration range of adsorption experiments. The pH of the metal ion solutions before and after kinetic or isotherm experiments was measured with a

combined ISE-H^+ glass electrode (Ross type 8102). The ISE-H^+ electrode was previously calibrated at the same experimental conditions of the adsorption experiments. To this end, 25 mL of standardized HNO_3 or HCl solution was titrated with NaOH by using a potentiometric titration system (Metrohm, Model 888 Titrando) controlled by the TIAMO software.

2.3. Models for kinetic and isotherm studies of Pb^{2+} adsorption

Kinetic data were first fitted with the pseudo-first order equation (PFO) of Lagergren (Yuh-Shan, 2004) (eq. 1) and the pseudo-second order equation (Blanchard, Maunaye, & Martin, 1984) (PSO, eq. 2):

$$\frac{dq_t}{dt} = k_1(q_e - q_t) \quad (1)$$

$$\frac{dq_t}{dt} = k_2(q_e - q_t)^2 \quad (2)$$

where q_t and q_e are the adsorption capacity of the adsorbent material (mg g^{-1}) at time t and at the equilibrium, respectively, k_1 (s^{-1}) and k_2 (g mg^{-1} s^{-1}) are the rate constants of adsorption. The relevant integrated forms of equations (1) and (2) are, respectively:

$$q_t = q_e\,(1 - e^{-k_1 t}) \quad (3)$$

$$q_t = \frac{q_e^2\, k_2\, t}{1 + q_e\, k_2 t} \quad (4)$$

However, as we will explain hereinafter, kinetic data were also subjected to a double exponential (DEM) regression analysis model according to the equation (5):

$$q_t = q_e[1 - \alpha \cdot e^{-k_1 t} - (1 - \alpha) \cdot e^{-k_2 t}] \quad (5)$$

where the parameter α accounts for the relative contribution of each exponential term to the overall adsorption amount ($0 < \alpha < 1$).

The adsorption equilibrium data have been processed according to the well-known Langmuir (Langmuir, 1918) (L, eq. 6) and Freundlich (Freundlich, 1907) (F, eq. 7) models:

$$q_e = \frac{q_m K_L c_e}{1+K_L c_e} \quad (6)$$

$$q_e = K_F c_e^{1/n} \quad (7)$$

where q_m (mg g^{-1}) is the maximum adsorption ability of the adsorbent, c_e (mg L^{-1}) is the Pb^{2+} concentration in solution at equilibrium; K_F ($L^{1/n}$ g^{-1} $mg^{1-1/n}$) and K_L ($L \cdot mg^{-1}$) are the constants of Freundlich and Langmuir models, respectively.

The Pb^{2+} ion adsorption capacity at different contact times t (q_t, mg g^{-1}) or at different Pb^{2+} / adsorbent ratios (q_e, mg g^{-1}) were calculated by the eq. 8:

$$q_t \text{ or } q_e = \frac{V (c_0 - c_t)}{m} \quad (8)$$

where V (L) is the volume of the metal ion solution and m is the mass of CyCaNS (g); c_0 and c_t are the Pb^{2+} ion concentrations in the solutions (mg L^{-1}) at $t = 0$ and $t = t$, respectively. At the equilibrium condition, eq. 7 was used by replacing c_t with c_e to calculate q_e.

The conditional Langmuir constant values (in $NaNO_3$ 0.1 mol L^{-1}, pH = 5.0; $c_{Pb^{2+}}$ in mol L^{-1}) (Yu Liu, 2009) in the temperature range 283.15 - 323.15 were used to calculate the thermodynamic parameters ΔG (kJ mol^{-1}), ΔH (kJ mol^{-1}) and ΔS (kJ mol^{-1} K^{-1}) by using Gibbs and van't Hoff equations (eqs 9 and 10). The following assumptions were done: *i*) the adsorption is reversible, *ii*) the stoichiometry of adsorption doesn't change; iii) equilibrium condition is established during adsorption experiments (Crini & Badot, 2008; Tran, You, & Chao, 2016).

$$\Delta G = -RT \ln K_L \quad (9)$$

$$\ln K_L = -\frac{\Delta H}{RT} + \frac{\Delta S}{R} \quad (10)$$

The LIANA, Kaleidagraph 4.0 and OriginLab suite software packages were used to perform fitting analyses of adsorption isotherms and kinetic data.

242

243 *2.4. FFC-NMR relaxometry*

244 Relaxometric experiments (Pellegrino Conte, 2019; Pellegrino Conte & Lo Meo, 2020; Paolo
245 Lo Meo et al., 2020) were performed with a STELAR SmarTracer apparatus at 3.0, 1.0 and 0.3
246 MHz, by applying a pre-polarized sequence. Samples of the nanosponges NS3 and NS4 (400 mg
247 each) were placed in a NMR tube (9 mm inner diameter) and equilibrated with a $NaNO_3$ 0.1 mol
248 L^{-1} solution adjusted at pH 5.0 by adding a small amount of HNO_3. Excess solution was carefully
249 pipetted out before relaxometric determinations. Analysis of relaxometrica data was performed
250 as described elsewhere (Paolo Lo Meo et al., 2020). In details, the T_1 relaxation kinetic data
251 recorded were first subjected to regression analysis according to equation (11):

252 $$I_t = I_0 + I_1 \cdot e^{-R_{fast}t} + I_2 \cdot e^{-R_{slow}t} \qquad (11)$$

253 where R_{fast} and R_{slow} account for the relaxation of water molecules residing at the solid-liquid
254 interface and flowing in the pores, respectively. Hence, the surface water fraction f_s can be
255 calculated according to the relationship (12):

256 $$f_s = (R_{slow} - R_w)/(R_{fast} - R_w) \qquad (12)$$

257 where R_w is the relaxation rate of bulk water. Relaxation kinetics were also subjected to
258 Inverse-Laplace transform analysis by means of the UPEN algorithm. The distributions obtained
259 were in turn decomposed as a sum of two Log-normal distributions, $F_{fast}(T_1)$ and $F_{slow}(T_1)$, from
260 which the PCI indexes were calculated according to equation (13):

261 $$PCI = \frac{\left(\int_{T_{A,fast}}^{T_{B,fast}} F_{fast}(T_1)T_1 dT_1\right)^{-1} - R_w}{\left(\int_{T_{A,slow}}^{T_{B,slow}} F_{slow}(T_1)T_1 dT_1\right)^{-1} - R_w} \qquad (13)$$

262 where the integration limits are defined as discussed in the reference work.

263

3. Results and Discussion

3.1. Speciation analysis

As a general rule, the percentages of protonated/unprotonated functional groups of the adsorbent material, and the percentages of all the species formed by the metal ion to be adsorbed at the experimental conditions of the treated aqueous solution as well, play an important role on the efficiency of adsorption process. Therefore, the knowledge of species distribution of both the adsorbent and the metal ion provides a necessary starting point to discuss the adsorption results properly, and to obtain information about the adsorption mechanisms. Thus, we preliminary performed a speciation study of the four CyCaNSs and the Pb^{2+} ion, by using the stability constants from literature. More in detail, the protonation constants of ionizable sites of the CyCaNSs had already been calculated in a previous work according to the Diprotic-Like Model (DLM (Crea et al., 2009)), in NaCl medium, at $I = 0.1$ mol L^{-1} and $T = 298.15$ K (see Supporting Information, Table S1) (Di Vincenzo et al., 2019). It is worth mentioning here that the average amount of ionizable groups in CyCaNSs determined by potentiometric titration techniques results significantly lower than that provided by solid-state NMR characterization. This peculiar finding was explained by admitting the existence of highly hydrophobic regions within the framework of the materials, which are hardly accessible to aqueous media.

The stability constants of Pb^{2+} species in NaCl, at different ionic strengths were taken from Cataldo et al. (Cataldo, Lando, et al., 2018), whilst the stability constants of hydrolytic species in $NaClO_4$ 0.1 mol L^{-1}, considered a non-interacting medium like $NaNO_3$, and at $I \rightarrow 0$ mol L^{-1} were taken from the references (Supporting Information, Table S2)(Baes & Mesmer, 1976). The speciation diagrams of CyCaNSs were drawn by using the concentrations of ionizable groups (triazole, amino and carboxyl groups) reported in Cataldo et al. (Cataldo, Lando, et al., 2018).

Conversely, those of Pb^{2+} were drawn at c_{Pb2+} = 30 mg L^{-1}, that was the initial concentration of the solution used in adsorption experiments.The percentages of Pb^{2+} and of CyCaNSs species formed at pH 3 and 5, calculated from the distribution diagrams drawn at the different experimental conditions are reported in Table 2 (see Figures 1S and 2S in the Supporting Information for complete details). The acid-base properties of the triazole unit of the CyCaNSs and of the amino unit of NS3 are well described by two protonation constants (di-functional units, according to the theory of DLM (Crea et al., 2009). Looking at the percentages of protonated and unprotonated species of CyCaNSs at pH 3 and 5, the only considerable variation regards the carboxylic units of NS4 (% of NS4-2 = 77.2 and 3.3 at pH 5 and 3, respectively). Also in the case of Pb^{2+} speciation, irrelevant differences were noted at the two pH values at the same experimental conditions. On the contrary, the concentration of chloride in metal ion solution completely changes the speciation of Pb^{2+} in the pH range 3~5 (e.g., % of Pb^{2+} = 99.8 and 24.3 at pH = 5.0, at I = 0.1 mol L^{-1}, in $NaClO_4$ and NaCl, respectively). The percent decrease for the aquo ion in solution containing NaCl background is due to the gradual increase of Pb-chloride complex species, in particular the positively charged $PbCl^+$ and the neutral $PbCl_2$, on increasing medium concentration.

3.2. Modelling of Pb^{2+} adsorption equilibria into NS3 and NS4 adsorbent materials

Preliminary adsorption tests, aimed at generally assessing the sorption abilities of the materials, enabled to select the best adsorbents to be used in further isotherm and kinetic experiments. We observed that pristine CyCaNSs NS1 and NS2 showed very poor performances. In fact, 8 % adsorption was found for NS1, whereas NS2 did not adsorb Pb^{2+} ion at all. Conversely, post-modified materials NS3 and NS4 were able to remove 70 % and 55 % of Pb^{2+} ion, respectively, under the conditions used (see Experimental).

Table 2. Percentage of CyCaNSs species and of Pb^{2+} species formed at pH = 5.0 and 3.0 (in parentheses), at T = 298.15 K

CyCaNSs	% of NSx-1 Species[a]			% of NSx-2 Species[b]		
	$(NSx\text{-}1)H_2$	(NSx-1)H	NSx-1	$(NSx\text{-}2)H_2$	(NSx-2)H	NSx-2
NS1	96 (100)[c]	4 (0)	0 (0)	-	-	-
NS2	96.1 (100)	3.9 (0)	0 (0)	-	-	-
NS3	-	97.7 (100)	2.3 (0)	99.9 (100)	0.1 (0)	0 (0)
NS4	99.7 (100)	0.3 (0)	0 (0)	-	22.8 (96.7)	77.2 (3.3)

Conditions	Pb^{2+}	$PbCl^+$	$PbCl_2$	$PbCl_3^-$	$Pb(OH)^+$
$I \rightarrow 0$ mol L^{-1}	99.8 (100)	-	-	-	0.2 (0)
$NaClO_4$ 0.1 mol L^{-1}	99.8 (100)	-	-	-	0.2 (0)
NaCl 0.01 mol L^{-1}	75.6 (76.2)	22.7 (22.9)	0.9 (0.9)	0 (0)	0.8 (0)
NaCl 0.05 mol L^{-1}	38.7 (39.1)	50.7 (51.3)	9.2 (9.3)	0.2 (0.2)	1.2 (0)
NaCl 0.1 mol L^{-1}	24.3 (24.5)	55.6 (56.0)	18.4 (18.5)	0.9 (0.9)	(0)

[a] triazole unit, in NaCl 0.1 mol L^{-1}; [b] amino or carboxyl unit, in NaCl 0.1 mol L^{-1}; [c] in parenthesis the percentages of species at pH = 3.

These observations are interesting because they indicate that the participation of possible $-NH_2$ or -COOH groups in the metal ion binding process is specifically involved. Moreover, this even implies that the other possible binding sites present in the materials, namely the secondary hydroxyl groups of the cyclodextrin subunits, the *soft* and electron-rich calixarene cavities and the electron-donor N atoms of the 1,2,4-triazole linkers, are not effective in accomplishing the Pb^{2+} ion binding process. Therefore, considering the affinity and the higher adsorption ability of

NS3 and NS4, the kinetic and thermodynamic studies were continued only on these latter two adsorbents.

The adsorption equilibria of NS3-Pb^{2+} and NS4-Pb^{2+} systems were studied in aqueous solution at different experimental conditions, namely, pH 3.0 and 5.0, at $I \rightarrow 0$ mol L^{-1} or with the addition of an ionic medium (either NaCl or $NaNO_3$) at different ionic strengths ($0.01 \leq I$ / mol $L^{-1} \leq 0.1$) and in the temperature range $283.15 \leq T$ / K ≤ 323.15. The experimental data, i.e. q_e vs c_e, have been fitted with both the Langmuir and Freundlich isotherm models. Typical trends are depicted in Figure 2 (the complete data plots are reported in the Supporting Information, Figures 3S-7S; the relevant fitting parameters are reported therein, Tables 3S – 6S).

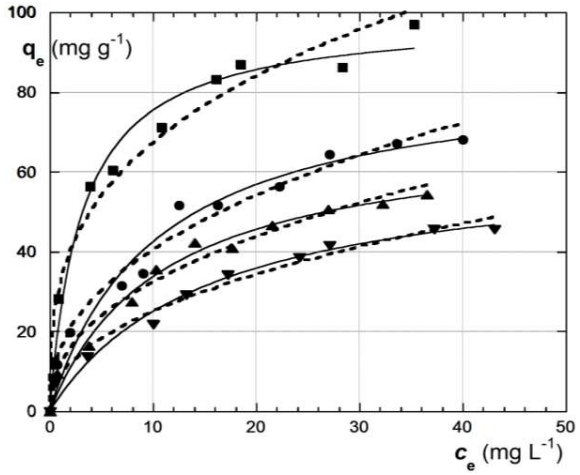

Figure 2. Adsorption isotherms of Pb^{2+} onto material NS4 from aqueous solutions at pH = 5.0 without ionic medium (■), in NaCl 0.01 (●), 0.05 (▲), 0.10 (▼) mol L^{-1} and at T = 295.15 K. Experimental data fitted with Langmuir (continuous lines) and Freundlich (dashed lines) models.

As a preliminary observation, better fitting quality was in general achieved by means of the Langumuir model, rather than with the Freundlich one. Although the satisfactory fitting of an isotherm does not necessarily give information on the mechanisms of the metal ion adsorption, it can be a useful parameter to predict or optimize the sorption processes. In fact, the calculation of

341 the Langmuir parameters K_L and q_m are related to the affinity of the material towards metal ion
342 and to the maximum amount of metal ion that is adsorbed. Noticeably, in batch experiments
343 carried out at pH = 5.0, we observed a decrease in the solution pH at equilibrium as large as ca.
344 0.8~1.2 units, depending on the amount of adsorbent used. This can be attributed to an ionic
345 exchange between the Pb^{2+} ions and the H^+ ions of protonated functional groups (i.e. - OH,
346 triazole, -NH_2 or –COOH) present in the CyCaNS materials, during the adsorption processes.
347 Conversely, when the starting pH was 3.0 no significant pH variation was found. Trends of the
348 of q_m, K_L , K_F and n_F values as a function of pH, nature of the ionic medium, ionic strength and
349 temperature are depicted as histograms in Figures 3 and 4.
350 For both adsorbent materials, the best adsorption capacities (q_m) and affinities (K_L) towards
351 Pb^{2+} were observed at pH 5.0 in the absence of the ionic medium. In details, q_m values as large as
352 114 mg g^{-1} for NS3 and 99 mg g^{-1} for NS4 are found, corresponding to 0.55 and 0.48 mmol g^{-1}
353 respectively. These results, in turn, can be compared with the amount of amine and carboxyl
354 groups present in the materials, obtained in a previous study by potentiometric titration, i.e. 0.68
355 and 0.75 mmol g^{-1} respectively (Di Vincenzo et al., 2019). It is worth recalling here that this
356 result was significantly lower than the theoretical amount of ionizable groups obtained from
357 solid state NMR characterization. This finding was explained by admitting the existence of
358 highly hydrophobic, non-water-accessible microdomains in the matrix. Hence, our results
359 provide good support to the aforementioned hypothesis.

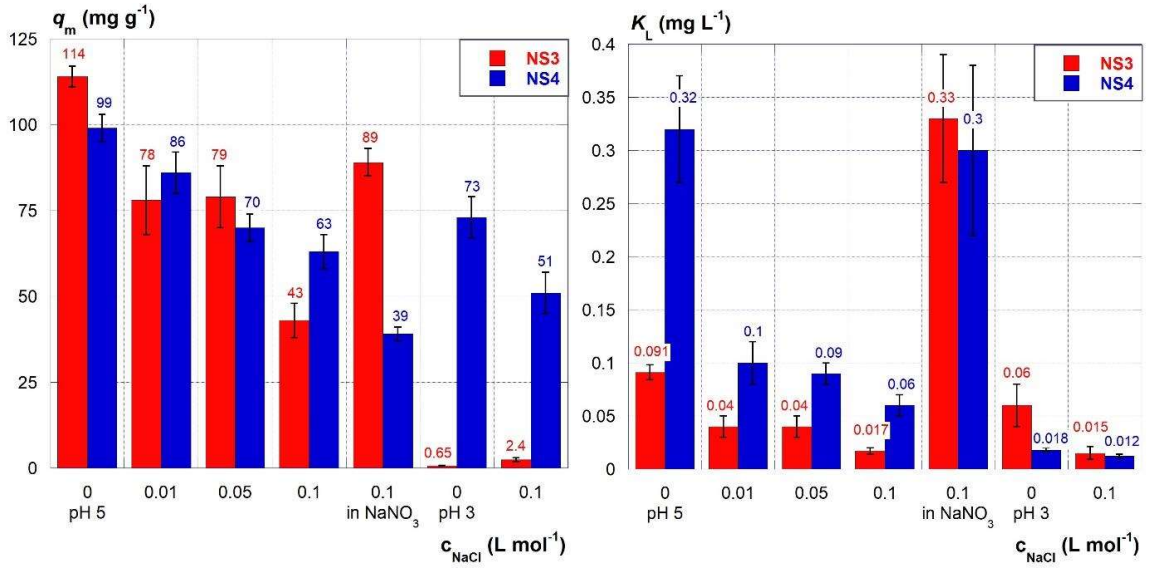

360

361 **Figure 3.** q_m (left) and K_L (right) values of Pb^{2+} adsorption onto NS3 and NS4 materials from
362 aqueous solutions at different experimental conditions: initial pH = 5.0, ionic medium NaCl or
363 $NaNO_3$; $0 \leq I$ /mol $L^{-1} \leq 0.1$; at $T = 298.15$ K.

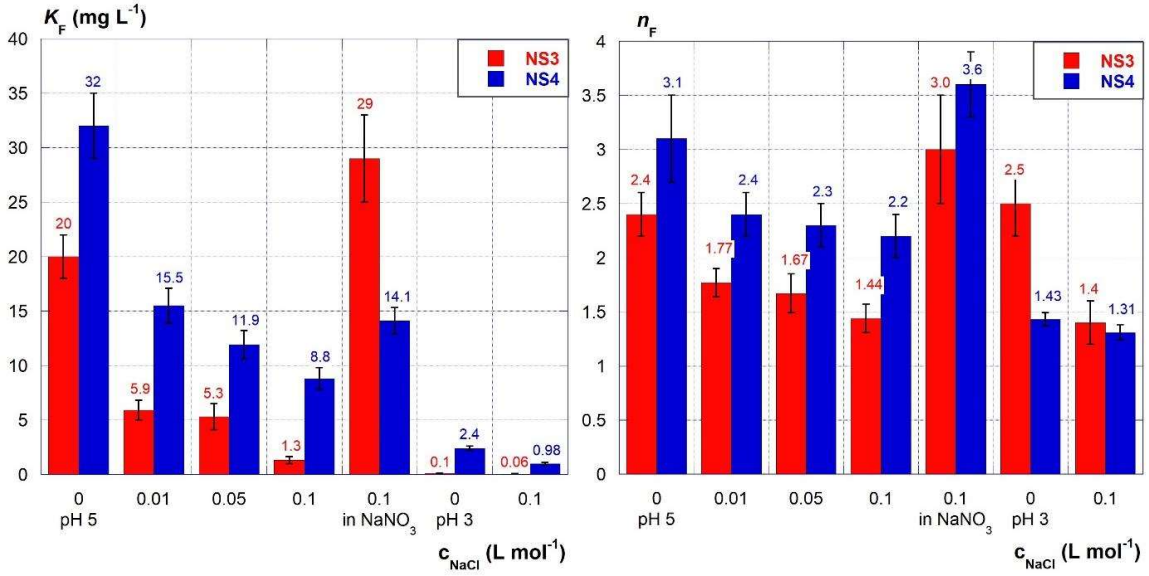

364

365 **Figure 4.** K_F (left) and n_F (right) values of Pb^{2+} adsorption onto NS3 and NS4 materials from
366 aqueous solutions at different experimental conditions: initial pH = 3.0 or 5.0, ionic medium =
367 NaCl or $NaNO_3$; $0 \leq I$ /mol $L^{-1} \leq 0.1$; at $T = 298.15$ K.

A noticeable decrease in q_m values occurs on going from pH 5.0 to pH 3.0. In fact, the NS3 adsorption ability almost drops down to zero, whereas the one for NS4 decreases to 73.4 at $I \rightarrow 0$ mol L^{-1}, and to 51.1 mg g^{-1} in NaCl 0.1 mol L^{-1}, respectively. It is worth recalling here that the variation of percentages of protonated/unprotonated NS3 and NS4 species and of Pb^{2+} species between pH 3 and 5 is almost negligible (see values reported in Table 1). Therefore, the reduction of the adsorption ability of NS3 and NS4 towards Pb^{2+} at pH = 3.0 may be ascribed to the higher H^+ concentration, which is in competition with Pb^{2+} in the feasible ion exchange adsorption mechanism.

Addition of NaCl to the solution causes a significant effect in the adsorption abilities (q_m) and affinities (K_L or K_F), both of which gradually decrease on increasing the concentration of the ionic medium. Again, it must be considered that NaCl causes negligible variations in the percentages of protonated/unprotonated forms of the adsorbent (e.g. through the formation of weak complexes between Na^+ and carboxylate groups of the nanosponge). Therefore, the observed decrease of the adsorption capacity can be confidently attributed to the decrease of the percent of the free aquo ion of lead, which is partly converted into complex chlorinated species (in particular $PbCl^+$ and $PbCl_2$, the percentages of which increase with chloride concentration, see Table 1). These species (in particular the neutral $PbCl_2$) have a lower affinity for the binding sites of the CyCaNSs. Moreover, in the case of NS3, the greater decrease in sorption ability with respect to NS4 can be attributed to the hydrochloride form of the $-NH_2$ groups, which contributes to hinder their interaction with the Pb^{2+} ions. These considerations are supported by the fact that affinities for Pb^{2+} (K_L and K_F) increase on changing the ionic medium from NaCl to $NaNO_3$, the ionic strength being equal (I = 0.1 mol L^{-1}). In particular, K_L and K_F values are on average about twenty and twenty-two times larger for NS3 and about five and two times larger for NS4, respectively.

391 The comparison between the two different CyCaNSs reveals interesting differences. At pH = 5
392 in the presence of NaCl, NS4 shows a better affinity than NS3 (K_L and K_F) towards the metal ion.
393 In particular, K_F values are on average ca. three times larger for NS4 than for NS3. On increasing
394 the NaCl concentration up to 0.1 mol L^{-1}, absorption capacities (q_m) decrease on a larger extent
395 for NS3 (62 %) than for NS4 (36 %). Noticeably, changing the ionic medium from NaCl to
396 $NaNO_3$ (I = 0.1 mol L^{-1}) causes an increase in the adsorption capacity for NS3, whereas the
397 opposite occurs for NS4. At the same time, a larger increase of K_L occurs for NS3 (ca. 20 times)
398 than for NS4 (ca. 5 times). Finally, comparison between data at I = 0 with those in the presence
399 of $NaNO_3$ at I = 0.1 mol L^{-1}, showed a large increase in the K_L value for NS3, whereas K_L was
400 substantially unchanged for NS4. All these observations outline, in general, a larger sensitivity to
401 environmental conditions for NS3 (as already observed for what concerns the effect of pH
402 variation). This is the effect of the different average charge status of the functional groups
403 present in the different materials (positive ammonium groups for NS3 vs. negative carboxylate
404 groups for NS4). In fact, neutral amine groups are less able than anionic carboxylate groups in
405 competing with water molecules and chloride ions for the positions in first coordination shell of
406 the metal ion. This finding is consistent with the fact that monocarboxylic acids possess a much
407 larger coordination ability towards Pb^{2+} ion (i.e. larger stability constants for complex formation)
408 than monoamines (Cataldo, Lando, et al., 2018). Therefore, the behavior differences between the
409 two CyCaNS discussed above can be ultimately justified on the grounds of the aforementioned
410 intrinsic coordination abilities of the functional groups, in perfect agreement with the well-
411 known reactivity-selectivity principle. Noticeably, the larger decrease in q_m values on changing
412 the ionic medium observed for NS4 can be also partly ascribed to a shielding effect of the Na^+
413 ion towards the anionic carboxylate groups, which does not occur for NS3.

414 *3.3. Thermodynamic parameters for Pb^{2+} adsorption onto NS3 and NS4.*

415 The study of the adsorption abilities of Pb^{2+} onto NS3 and NS4 at equilibrium was
416 complemented by the estimation of the relevant thermodynamic parameters ΔG, ΔH and ΔS,
417 which was performed by applying Gibbs and van't Hoff equations to the data recorded at
418 different temperatures (in the range 283.15~323.15 K). Data are collected in Table 3 and
419 depicted in Figure 5.

420 For both materials, the metal ion adsorption is a spontaneous process (negative ΔG values) in
421 the temperature range explored. Adsorption capacities of both NS3 and NS4 undergo only minor
422 decrease on increasing the temperature. A similar, but more noticeable trend occurs for K_L
423 values. Consequently, the adsorption process results to be exothermic, with a small and positive
424 entropy variation ($\Delta H°$ = -18 and -11.4 kJ mol^{-1}, $\Delta S°$ = 25 and 4 J mol^{-1} K^{-1} for NS3 and NS4,
425 respectively). The occurrence of positive ΔS values suggests a structural changing in the
426 adsorbent and an increasing randomness at the adsorbent – solution interfaces (Aksu, 2002; Yu
427 Liu & Liu, 2008; Tran et al., 2016). In the temperature range investigated, the ΔG values vary in
428 the ranges -26.5 – -28.6 and -26.8 – -28.0 kJ mol^{-1} for NS4 and NS3, respectively, which are
429 comparable with other literature data (El-Kafrawy, El-Saeed, Farag, El-Saied, & Abdel-Raouf,
430 2017). Indeed, ΔG values in the range -20~80 kJ mol^{-1} are considered typical of an adsorption
431 based on ion exchange (Gereli, Seki, Murat Kuşoğlu, & Yurdakoç, 2006; Önal, Akmil-Başar, &
432 Sarıcı-Özdemir, 2007; Tran et al., 2016). Therefore, also ΔG values suggest an ion exchange
433 mechanism, which is in perfect agreement with hypothesis done on the basis of acid-base
434 properties of binding groups of NS3 and NS4 and of the Pb^{2+} species present in the aqueous
435 solution at the studied experimental conditions.
436

Table 3. Thermodynamic parameters ΔG, ΔH and ΔS for the Pb^{2+} adsorption onto NS3 and NS4 from aqueous solution at pH = 5, in $NaNO_3$,at I = 0.1 mol L^{-1} , in the temperature range 283.15~323.15 K.

Adsorbent	T (K)	q_e [a]	$-\Delta G$ [b]	ΔH [b]	ΔS [c]
NS3	283.15	92.9 ± 3.9	26.8 ± 0.2	-18 ± 3	25 ± 9
	295.15	88.8 ± 4.3	27.3 ± 0.3		
	308.15	86.6 ± 6.1	28.0 ± 0.5		
	323.15	81.0 ± 4.2	28.0± 0.5		
NS4	283.15	37.6 ± 1.9	26.5 ± 0.5	-11.4 ± 0.8	4 ± 3
	295.15	39.4 ± 2.2	27.1 ± 0.5		
	308.15	34.9 ± 2.5	27.9 ± 0.4		
	323.15	32.0 ± 2.8	28.6 ± 0.4		

[a] mg g^{-1}, ± std. dev.; [b] kJ mol $^{-1}$, ± std. dev.; [c] J mol $^{-1}$ K^{-1}, ± std. dev.

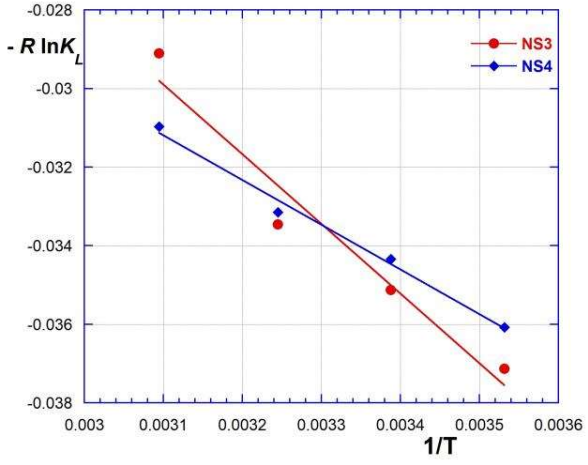

Figure 5. plot of $-R\ln K_L$ vs. 1/T for the calculation of thermodynamic parameters ΔH and ΔS for Pb^{2+} adsorption onto NS4 at pH = 5.0, in $NaNO_3$ 0.1 mol L^{-1}, by using van't Hoff equation.

3.4. Kinetics of Pb^{2+} adsorption onto NS3 and NS4.

The kinetics of Pb^{2+} adsorption onto NS3 and NS4 was studied at pH = 5.0, in $NaNO_{3aq}$ at I = 0.1 mol L^{-1} and T = 298.15 K. In both kinetic experiments were used the same amount of adsorbent, i.e. ca 15 mg, and the same metal ion solution (20 mL, c_{Pb2+} = 35 mg L^{-1}). Relevant data are illustrated in Figure 6. The PFO and PSO kinetic models were first used to fit the experimental data. However, visual observation of the data plots suggested us to use also a double-exponential DEM fitting model as a suitable alternative. Fitting parameters obtained are collected in Table 4. A quick overview of results collected in Table 4 clearly shows that the PFO model affords an inferior fitting of experimental data. Conversely, in both cases, statistical testing parameters indicated that the DEM model was the best model. The latter finding is interesting, because it mirrors the kinetic profiles observed for the release of some organic guests from CyCaNSs composites.(Guernelli, Cariola, Baschieri, Amorati, & Lo Meo, 2020; Massaro et al., 2016) This suggests the idea that adsorption occurs through the superimposition of two different processes, a "fast" and a "slow" one, probably accounting for the occurrence of mass transfer phenomena within the material texture.

Both the PSO and the DEM models agree in indicating that NS4 is faster than NS3 in accomplishing adsorption. More in detail, as long as the PSO model is concerned, k_2 is ca. 2.5 times larger for the former material. For the DEM model, k_1 and k_2 result ca. 4 times and 3 times larger, respectively. Conversely, NS3 shows a much larger adsorption capacity (ca. 3 times) than NS4. It is worth noting, at this purpose, that the value for the α parameter found in the case of NS3 (i.e. 0.87) suggests that most of the metal ion is absorbed during the "fast" step of the process. Differently, the α value for NS4 (0.44) indicates that both steps equally contribute to overall adsorption.

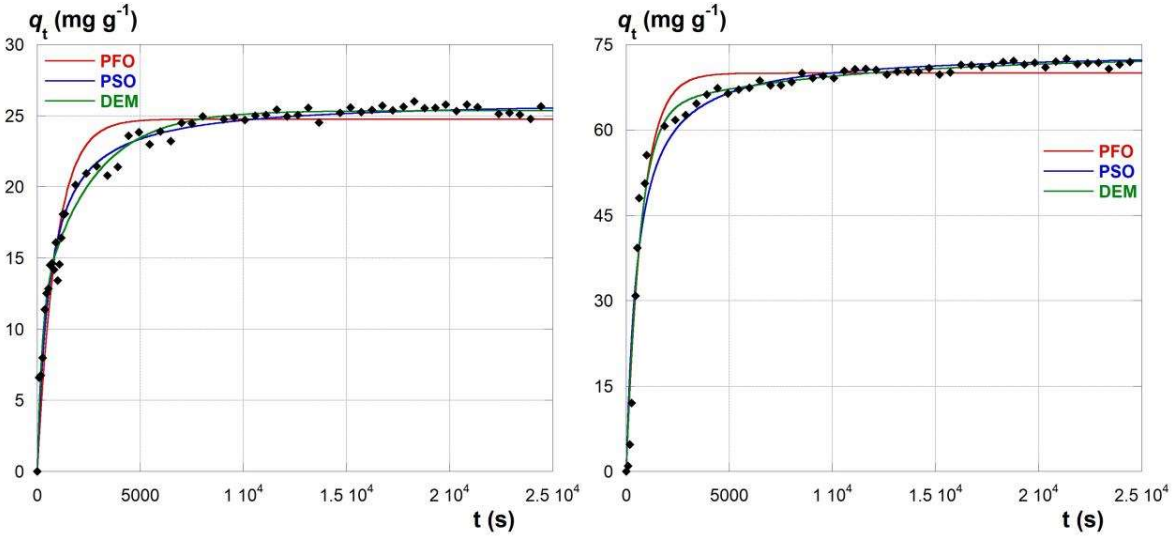

469

470 **Figure 6.** Dependence of q_t (mg g $^{-1}$) on contact time for the Pb^{2+} adsorption onto NS3 (left) and

471 NS4 (right). Data were fitted with the PFO (red), PSO (blue) and DEM (green) kinetic models.

472 **Table 4.** Parameters of PFO and PSO and DEM kinetic equations for Pb^{2+} adsorption onto NS4

473 anNS3 in aqueous solution at pH = 5.0, in $NaNO_3$, at I = 0.1 mol L^{-1} and T = 298.15 K

material	PFO	PSO	DEM
NS3	$q_e = 69.9 \pm 0.5$ mg g^{-1} $k_1 = (1.30 \pm 0.07)\cdot10^{-3}$ s^{-1} $R^2 = 0.9618$	$q_e = 73.8 \pm 0.7$ mg g^{-1} $k_2 = (2.5 \pm 0.2)\cdot10^{-5}$ s^{-1} mg^{-1} g $R^2 = 0.9649$	$q_e = 72.7 \pm 1.8$ mg g^{-1} $\alpha = 0.87 \pm 0.03$ $k_1 = (1.53 \pm 0.12)\cdot10^{-3}$ s^{-1} $k_2 = (1.0 \pm 0.7)\cdot10^{-4}$ s^{-1} $R^2 = 0.9781$
NS4	$q_e = 24.7 \pm 0.3$ mg g^{-1} $k_1 = (1.10 \pm 0.06)\cdot10^{-3}$ s^{-1} $R^2 = 0.9421$	$q_e = 26.1 \pm 0.2$ mg g^{-1} $k_2 = (6.4 \pm 0.3)\cdot10^{-5}$ s^{-1} mg^{-1} g $R^2 = 0.9813$	$q_e = 25.3 \pm 0.2$ mg g^{-1} $\alpha = 0.44 \pm 0.03$ $k_1 = (4.7 \pm 0.7)\cdot10^{-3}$ s^{-1} $k_2 = (4.0 \pm 0.4)\cdot10^{-4}$ s^{-1} $R^2 = 0.9858$

474

As a final remark, it is worth noting that, as long as the PSO model is concerned, the k_2 values found in our case appear a little lower in comparison with other literature reports (Taka, Fosso-Kankeu, Pillay, & Mbianda, 2018; Zhao et al., 2019).

3.5. Textural features of NS3 and NS4 from FFC-NMR relaxometry.

In order to rationalize the whole of the experimental results, we reasoned that, along with the different chemical functionalization of the materials, the relevant physico-chemical and morphological features should be accounted for, with particular regard to their permeability to aqueous media. At this purpose, it is worth mentioning here that the textural/porosimetric properties of nanosponges can be hardly investigated with the ordinary BET/BJH methodologies (L. D. Wilson, Mohamed, & Berhaut, 2011; Lee D. Wilson, Mohamed, & Headley, 2011), whereas interesting and valuable information can be achieved by means of fast-field cycling (FFC) NMR relaxometric techniques. Investigation of the ^{1}H longitudinal relaxation for a micro- or nano-porous material sample saturated with water, enables to evaluate the fraction f_s of water molecules directly interacting with the pore surface (Bird, Preston, Randall, Whalley, & Whitmore, 2005; Pohlmeier, Haber-Pohlmeier, & Stapf, 2009; Stingaciu et al., 2010). Moreover, the inverse-Lagrange transform of the relaxation kinetics data can be correlated with pore size distribution (P. Conte & Ferro, 2018; Pellegrino Conte & Ferro, 2020). In the case of materials such as nanosponges, which may undergo swelling in the presence of aqueous media, a "*pore connectivity index*" (*PCI*) can be defined, in order to to describe the functional mobility of water within the nanopore network (Paolo Lo Meo et al., 2020).

We studied the longitudinal relaxation of materials NS3 and NS4 at three Larmor frequencies (3, 1 and 0.3 MHz) after equilibration with aqueous $NaNO_3$ 0.1 mol L^{-1} solution at pH 5.0.

According to previous literature, relaxation kinetics follows a double-exponential trend, with a "fast" and a "slow" component accounting for the relaxation of water molecules interacting with the pore surface or flowing in the nano-channels (a typical trend is shown in Figure 7). Accordingly, the relevant inverse-Laplace transform can be fitted as a sum of two Log-normal distributions. Relaxometric data (see Experimental for details) are summarized in Table 5.

Table 5. Summary of FFC-NMR relaxometric data.

	NS3				**NS4**			
ω_L (MHz)	R_{fast} (μs^{-1})	R_{slow} (μs^{-1})	f_s	*PCI*	R_{fast} (μs^{-1})	R_{slow} (μs^{-1})	f_s	*PCI*
3.0	110 ± 40	45 ± 7	0.40		67 ± 8	18 ± 3	0.27	
1.0	140 ± 40	54 ± 7	0.40	1.66	98 ± 8	29 ± 2	0.29	2.07
0.3	170 ± 60	61 ± 6	0.36		88 ± 5	26 ± 2	0.30	

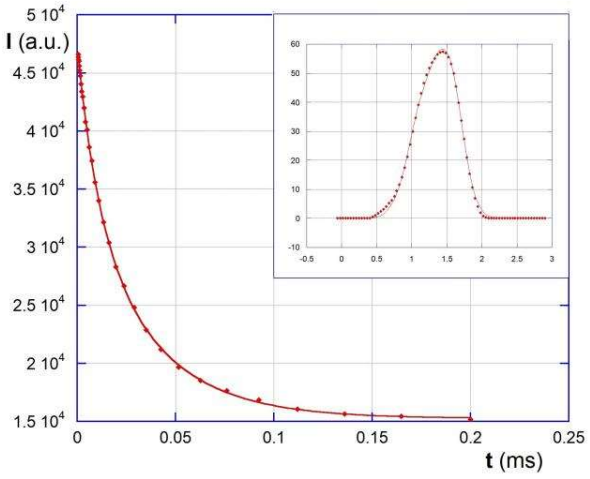

Figure 7. T1 relaxation kinetics for NS4 at 1.0 MHz; in inset the relevant Inverse-Laplace transform (UPEN).

509

510 The results indicate a smaller fraction of pore surface water molecules and a larger *PCI* value
511 for NS4 than for NS3. Keeping into account the presence in the CyCaNSs of two different co-
512 monomer units (i.e., the hydrophilic cyclodextrin and the hydrophobic calixarene), these results
513 suggest that NS3 can be more extensively permeated by the aqueous medium than NS4. This is
514 consistent with the presence in its composition of a larger amount of cyclodextrin, which can
515 effectively interact with the medium via H-bonds by means of the –OH groups therein. Because
516 of this, however, the medium perceives a better mobility in the nanochannels of the most
517 hydrophobic material NS4, in agreement with the its faster adsorption kinetics.

518

519 *3.6. Recycle and reuse of the absorbent materials.*

520 The possibility of recycling an adsorbent material, makes its application more attractive,
521 because of possible lowering of the costs for polluted water treatment. Therefore, recycle and
522 reuse experiments were carried out on both NS3 and NS4 making for each of them four
523 adsorption/desorption steps (see Experimental for details). A 0.1 mol L^{-1} HNO_3 solution was
524 used as the extraction medium; the results of the four cycles are depicted in Figure 8.

525 The NS4 material showed an excellent reuse capacity with comparable and constant q_e values
526 of adsorption and desorption in each of the four cycle. This result is perfectly consistent with the
527 ion exchange mechanism hypothesized previously. Nevertheless, the adsorption and desorption
528 of the metal ion may probably be also ascribed to a combination of chemical and physical
529 processes, the outcome of which varies according to the experimental conditions of the aqueous
530 solution containing the metal ion. The results obtained for NS3 are quite different. Apparently,
531 the material showed a scarce reuse capacity. In fact, even in the first desorption step the amount

of recovered metal is lower than the amount of adsorbed one. Then, a dramatic drop in the adsorption capacity occurred, even since the second cycle. Again, for each cycle we observed that the amount of recovered metal is lower than the adsorbed one, and similar results are obtained in subsequent cycles. This unsatisfactory result suggests that some significant structural alteration or degradation occur in the material, after having interacted for the first time with the Pb^{2+} ion, which can be likely ascribed to the peculiar chemical behavior of the primary amine groups present

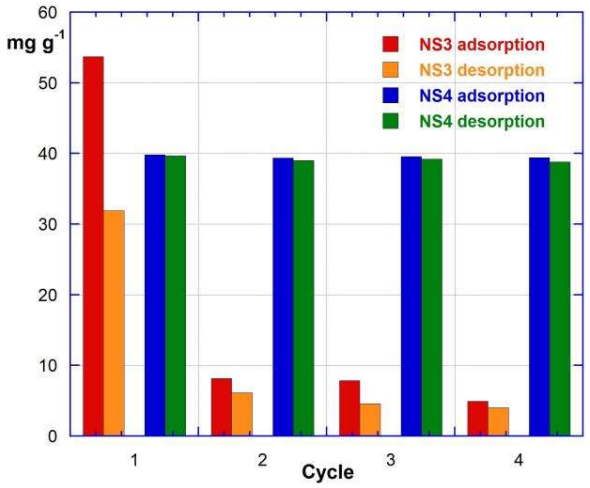

Figure 8. q_e values of Pb^{2+} adsorption and desorption steps in recycle experiments with NS3 and NS4. Experimental details: amount of CyCaNSs in column = 12.1 mg (NS3), 10.2 mg (NS4); treated solution: V = 20 mL; c_{Pb2+} = 35 mg L^{-1}; pH = 5.0; extracting solution: HNO_3 0.1 mol L^{-1}.

4. Conclusions and further remarks

Four pre- and post-modified cyclodextrin-calixarene nanosponges (CyCaNSs) have been employed as adsorbents for Pb^{2+} ions from aqueous solutions. Preliminary adsorption tests showed very poor performances of the NS1 and NS2 materials; conversely, the post-modified

materials NS3 and NS4, functionalized with amino and carboxyl groups, respectively, showed a very good affinity and adsorption ability towards the metal ion. Then, several batch kinetic and thermodynamic experiments were carried out in order to study the adsorption performances of NS3 and NS4 as function of ionic medium ($NaNO_3$, NaCl), ionic strength ($0 \leq I$ / mol $L^{-1} \leq 0.1$), pH (3.0, 5.0) and temperature ($283.15 \leq T$ / K ≤ 323.15). Our materials showed the highest adsorption ability at pH = 5.0 (q_m = 114 and 99 mg g^{-1} at $I \rightarrow 0$ mol L^{-1} for NS3 and NS4, respectively). The addition of NaCl to the metal ion solution causes a lowering of their adsorption ability (q_m) and affinity (K_L, K_F) mainly attributable to the formation of chloride species of Pb^{2+} ions. Moreover, the hydrochloride form of amino groups of NS3, especially at pH 3.0, hinders their interaction with the metal ion causing a higher lowering of adsorption parameters. The addition of $NaNO_3$ causes, in general, a smaller reduction of the adsorption capacity that, however, is more pronounced for NS4 suggesting a shielding effect of the Na^+ ions towards the anionic carboxylate groups of the adsorbent. The negative ΔG values confirm that the adsorption onto both materials is a spontaneous process predominantly based on ion exchange mechanism. Moreover, it is exothermic with low and positive entropy variations suggesting a structural changing in the adsorbents and an increasing randomness at the adsorbent – solution interfaces. For both post modified CyCaNSs, statistical testing parameters agree in indicating the DEM model as the best kinetic equation in terms of data fit. NS4 is faster than NS3 in accomplishing adsorption with k_1 and k_2 values about 4 times and 3 times larger respectively. The later result can be rationalized in terms of a better functional mobility of water within the nanopores of the nanosponge matrix, as accounted for by the relaxometric determinations. Finally, the NS4 material showed an excellent reuse capacity with comparable

571 adsorption and desorption abilities in each of the four cycles. By contrast, worse reuse
572 performances were shown by NS3.
573 As a final remark, we can also conclude that our CyCaNSs actually appear interesting and
574 promising materials for environmental remediation purposes. Indeed, their ability in
575 sequestrating organic pollutants has been already accounted for elsewhere (Cinà et al., 2017; P.
576 Lo Meo et al., 2014). Here we positively showed the possibility to extend their use to inorganic
577 pollutants at the same time. It is worth noting here that, as long as adsorption capacities (q_m) are
578 concerned, the performances of materials NS3 and NS4 appear comparable or even better to
579 other recent literature reports on cyclodextrin-based materials (El-Kafrawy et al., 2017; Li et al.,
580 2020; Rubin Pedrazzo et al., 2019; Taka et al., 2018; Zhao et al., 2019; Zheng et al., 2019), and
581 even superior to materials such as activated carbon (M. M. Rao, Ramana, Seshaiah, Wang, &
582 Chien, 2009), iron oxide (Nassar, 2010) or carbon nitride (Hu et al., 2015). Of course, further
583 studies are needed to investigate the sequestration of different metal species and the molecular
584 mechanisms involved in the process.
585
586 **Supporting Information**. Protonation constants of ionisable groups of CyCaNSs; Formation
587 constants of Pb^{2+} species in aqueous solutions; Langmuir and Freundlich isotherm parameters for
588 the Pb^{2+} adsorption onto CyCsNSs; Distribution diagrams of the NSx-1 and NSx-2 species vs pH
589 and Adsorption isotherms are reported.
590
591 ACKNOWLEDGMENTS

University of Palermo is gratefully acknowledged for financial support.
593

REFERENCES

Aksu, Z. (2002). Determination of the equilibrium, kinetic and thermodynamic parameters of the batch biosorption of nickel(II) ions onto Chlorella vulgaris. *Process Biochemistry,* 38(1), 89-99.

Allahyari, S., Trotta, F., Valizadeh, H., Jelvehgari, M., & Zakeri-Milani, P. (2019). Cyclodextrin-based nanosponges as promising carriers for active agents. *Expert Opinion on Drug Delivery,* 16(5), 467-479.

Baes, C. F., & Mesmer, R. E. (1976). *The Hydrolysis of Cations*.

Bird, N. R. A., Preston, A. R., Randall, E. W., Whalley, W. R., & Whitmore, A. P. (2005). Measurement of the size distribution of water-filled pores at different matric potentials by stray field nuclear magnetic resonance. *European Journal of Soil Science,* 56(1), 135-143.

Blanchard, G., Maunaye, M., & Martin, G. (1984). Removal of heavy metals from waters by means of natural zeolites. *Water Research,* 18(12), 1501-1507.

Bonomo, R. P., Pedotti, S., Vecchio, G., & Rizzarelli, E. (1996). Molecular Recognition of Amino Acids by Copper(II) Complexes of 6A,6X-Diamino-6A,6X-dideoxy-β-cyclodextrin (X = B, C, D). *Inorganic Chemistry,* 35(23), 6873-6877.

Bose, P. K., & Polavarapu, P. L. (1999). Evidence for covalent binding between copper ions and cyclodextrin cavity: a vibrational circular dichroism study. *Carbohydrate Research,* 323(1), 63-72.

Caldera, F., Tannous, M., Cavalli, R., Zanetti, M., & Trotta, F. (2017). Evolution of Cyclodextrin Nanosponges. *International Journal of Pharmaceutics,* 531(2), 470-479.

615 Cataldo, S., Cavallaro, G., Gianguzza, A., Lazzara, G., Pettignano, A., Piazzese, D., &
616 Villaescusa, I. (2013). Kinetic and equilibrium study for cadmium and copper removal from
617 aqueous solutions by sorption onto mixed alginate/pectin gel beads. *Journal of Environmental*
618 *Chemical Engineering,* 1(4), 1252-1260.

619 Cataldo, S., Chiodo, V., Crea, F., Maisano, S., Milea, D., & Pettignano, A. (2018). Biochar from
620 byproduct to high value added material – A new adsorbent for toxic metal ions removal from
621 aqueous solutions. *Journal of Molecular Liquids,* 271, 481-489.

622 Cataldo, S., Gianguzza, A., Pettignano, A., & Villaescusa, I. (2013). Mercury(II) removal from
623 aqueous solution by sorption onto alginate, pectate and polygalacturonate calcium gel beads. A
624 kinetic and speciation based equilibrium study. *Reactive and Functional Polymers,* 73(1), 207-
625 217.

626 Cataldo, S., Lando, G., Milea, D., Orecchio, S., Pettignano, A., & Sammartano, S. (2018). A
627 novel thermodynamic approach for the complexation study of toxic metal cations by a landfill
628 leachate. *New Journal of Chemistry,* 42(10), 7640-7648.

629 Cavalli, R., Trotta, F., & Tumiatti, W. (2006). Cyclodextrin-based Nanosponges for Drug
630 Delivery. *Journal of inclusion phenomena and macrocyclic chemistry,* 56(1), 209-213.

631 Chilajwar, S. V., Pednekar, P. P., Jadhav, K. R., Gupta, G. J. C., & Kadam, V. J. (2014).
632 Cyclodextrin-based nanosponges: a propitious platform for enhancing drug delivery. *Expert*
633 *Opinion on Drug Delivery,* 11(1), 111-120.

634 Cinà, V., Russo, M., Lazzara, G., Chillura Martino, D., & Lo Meo, P. (2017). Pre- and post-
635 modification of mixed cyclodextrin-calixarene co-polymers: A route towards tunability.
636 *Carbohydrate Polymers,* 157, 1393-1403.

637 Conte, P. (2019). *Chapter 10 Environmental Applications of Fast Field-cycling NMR*
638 *Relaxometry*. In *Field-cycling NMR Relaxometry: Instrumentation, Model Theories and*
639 *Applications* (pp. 229-254): The Royal Society of Chemistry

640 Conte, P., & Ferro, V. (2018). Measuring hydrological connectivity inside a soil by low field
641 nuclear magnetic resonance relaxometry. *Hydrological Processes,* 32(1), 93-101.

642 Conte, P., & Ferro, V. (2020). Standardizing the use of fast-field cycling NMR relaxometry for
643 measuring hydrological connectivity inside the soil. *Magnetic Resonance in Chemistry,* 58(1), 41-
644 50.

645 Conte, P., & Lo Meo, P. (2020). Nuclear Magnetic Resonance with Fast Field-Cycling Setup: A
646 Valid Tool for Soil Quality Investigation. *Agronomy,* 10(7), 1040.

647 Crea, F., De Stefano, C., Gianguzza, A., Pettignano, A., Piazzese, D., & Sammartano, S. (2009).
648 Acid−Base Properties of Synthetic and Natural Polyelectrolytes: Experimental Results and Models
649 for the Dependence on Different Aqueous Media. *Journal of Chemical & Engineering Data,* 54(2),
650 589-605.

651 Crini, G., & Badot, P.-M. (2008). Application of chitosan, a natural aminopolysaccharide, for
652 dye removal from aqueous solutions by adsorption processes using batch studies: A review of
653 recent literature. *Progress in Polymer Science,* 33(4), 399-447.

654 Crompton, T. R. (2007). *Toxicants in aqueous ecosystems: A guide for the analytical and*
655 *environmental chemist*.

656 Di Vincenzo, A., Russo, M., Cataldo, S., Milea, D., Pettignano, A., & Lo Meo, P. (2019). Effect
657 of pH Variations on the Properties of Cyclodextrin-Calixarene Nanosponges. *ChemistrySelect,*
658 4(20), 6155-6161.

659 El-Kafrawy, A. F., El-Saeed, S. M., Farag, R. K., El-Saied, H. A. A., & Abdel-Raouf, M. E. S.
660 (2017). Adsorbents based on natural polymers for removal of some heavy metals from aqueous
661 solution. *Egyptian Journal of Petroleum,* 26(1), 23-32.

662 Fontana, R. M., Milano, N., Barbara, L., Di Vincenzo, A., Gallo, G., & Meo, P. L. (2019).
663 Cyclodextrin-Calixarene Nanosponges as Potential Platforms for pH-Dependent Delivery of
664 Tetracycline. *ChemistrySelect,* 4(33), 9743-9747.

665 Freundlich, H. (1907). Über die Adsorption in Lösungen. *Zeitschrift fur Physikalische Chemie,*
666 57U(1), 385.

667 Gereli, G., Seki, Y., Murat Kuşoğlu, İ., & Yurdakoç, K. (2006). Equilibrium and kinetics for the
668 sorption of promethazine hydrochloride onto K10 montmorillonite. *Journal of Colloid and*
669 *Interface Science,* 299(1), 155-162.

670 Gidlow, D. A. (2015). Lead toxicity. *Occupational Medicine,* 65(5), 348-356.

671 Guernelli, S., Cariola, A., Baschieri, A., Amorati, R., & Lo Meo, P. (2020). Nanosponges for the
672 protection and release of the natural phenolic antioxidants quercetin, curcumin and phenethyl
673 caffeate. *Materials Advances,* 1(7), 2501-2508.

Hu, R., Wang, X., Dai, S., Shao, D., Hayat, T., & Alsaedi, A. (2015). Application of graphitic carbon nitride for the removal of Pb(II) and aniline from aqueous solutions. *Chemical Engineering Journal,* 260, 469-477.

Julinová, M., & Slavík, R. (2012). Removal of phthalates from aqueous solution by different adsorbents: A short review. *Journal of Environmental Management,* 94(1), 13-24.

Karoyo, A. H., & Wilson, L. D. (2015). Nano-Sized cyclodextrin-based molecularly imprinted polymer adsorbents for perfluorinated compounds—a mini-review. *Nanomaterials,* 5(2), 981-1003.

Khan, A. R. F., P.; Stine, K. J.; D'Souza, V. T. . (1998). Methods for Selective Modifications of Cyclodextrins. *Chemical Reviews,* 98(5), 1977.

Langmuir, I. (1918). The adsorption of gases on plane surfaces of glass, mica and platinum. *Journal of the American Chemical Society,* 40(9), 1361-1403.

Li, L., Chen, B., Su, Z., Wu, J., Pan, Z., & Fu, Z. (2020). Preparation of cyclodextrin-modified graphene oxide and its adsorption properties for Pb (II). *IOP Conference Series: Earth and Environmental Science* (5 ed., Vol. 446).

Liu, J., Mendoza, S., Román, E., Lynn, M. J., Xu, R., & Kaifer, A. E. (1999). Cyclodextrin-Modified Gold Nanospheres. Host−Guest Interactions at Work to Control Colloidal Properties. *Journal of the American Chemical Society,* 121(17), 4304-4305.

Liu, J., Ong, W., Kaifer, A. E., & Peinador, C. (2002). A "Macrocyclic Effect" on the Formation of Capped Silver Nanoparticles in DMF. *Langmuir,* 18(16), 5981-5983.

694 Liu, J., Ong, W., Román, E., Lynn, M. J., & Kaifer, A. E. (2000). Cyclodextrin-Modified Gold
695 Nanospheres. *Langmuir,* 16(7), 3000-3002.

696 Liu, Y. (2009). Is the Free Energy Change of Adsorption Correctly Calculated? *Journal of*
697 *Chemical & Engineering Data,* 54(7), 1981-1985.

698 Liu, Y., Liu, M., Jia, J., Wu, D., Gao, T., Wang, X., Janyong, Y., Li, F. (2019). β-Cyclodextrin-
699 based hollow nanoparticles with excellent adsorption performance towards organic and inorganic
700 pollutants. *Nanoscale,* 11(40), 18653-18661.

701 Liu, Y., & Liu, Y.-J. (2008). Biosorption isotherms, kinetics and thermodynamics. *Separation*
702 *and Purification Technology,* 61(3), 229-242.

703 Lo Meo, P., Lazzara, G., Liotta, L., Riela, S., & Noto, R. (2014). Cyclodextrin-calixarene co-
704 polymers as a new class of nanosponges. *Polymer Chemistry,* 5(15), 4499-4510.

705 Lo Meo, P., Mundo, F., Terranova, S., Conte, P., & Chillura Martino, D. (2020). Water
706 Dynamics at the Solid–Liquid Interface to Unveil the Textural Features of Synthetic Nanosponges.
707 *The Journal of Physical Chemistry B,* 124(9), 1847-1857.

708 Mason, L. H., Harp, J. P., & Han, D. Y. (2014). Pb Neurotoxicity: Neuropsychological Effects
709 of Lead Toxicity. *BioMed Research International,* 2014, 840547.

710 Massaro, M., Cina, V., Labbozzetta, M., Lazzara, G., Lo Meo, P., Poma, P., Riela, S., Noto, R.
711 (2016). Chemical and pharmaceutical evaluation of the relationship between triazole linkers and
712 pore size on cyclodextrin-calixarene nanosponges used as carriers for natural drugs. *RSC*
713 *Advances,* 6(56), 50858-50866.

714 Massoud, R., Hadiani, M. R., Hamzehlou, P., & Khosravi-Darani, K. (2019). Bioremediation of
715 heavy metals in food industry: Application of Saccharomyces cerevisiae. *Electronic Journal of*
716 *Biotechnology,* 37, 56-60.

717 Meldal, M., & Tornøe, C. W. (2008). Cu-Catalyzed Azide−Alkyne Cycloaddition. *Chemical*
718 *Reviews,* 108(8), 2952-3015.

719 Morin-Crini, N., & Crini, G. (2013). Environmental applications of water-insoluble β-
720 cyclodextrin–epichlorohydrin polymers. *Progress in Polymer Science,* 38(2), 344-368.

721 *Nanosponges: Synthesis and Applications*. (2019). Weinheim, Germany: Wiley- VCH Verlag
722 GmbH & Co. KGaA.

723 Nassar, N. N. (2010). Rapid removal and recovery of Pb(II) from wastewater by magnetic
724 nanoadsorbents. *Journal of Hazardous materials,* 184(1), 538-546.

725 Noël, S., Léger, B., Ponchel, A., Philippot, K., Denicourt-Nowicki, A., Roucoux, A., & Monflier,
726 E. (2014). Cyclodextrin-based systems for the stabilization of metallic(0) nanoparticles and their
727 versatile applications in catalysis. *Catalysis Today,* 235, 20-32.

728 Oliveri, V., Pietropaolo, A., Sgarlata, C., & Vecchio, G. (2017). Zinc Complexes of
729 Cyclodextrin-bearing 8-Hydroxyquinoline Ligands: A Comparative Study. *Chemistry – An Asian*
730 *Journal,* 12(1), 110-115.

731 Önal, Y., Akmil-Başar, C., & Sarıcı-Özdemir, Ç. (2007). Elucidation of the naproxen sodium
732 adsorption onto activated carbon prepared from waste apricot: Kinetic, equilibrium and
733 thermodynamic characterization. *Journal of Hazardous materials,* 148(3), 727-734.

734 Pohlmeier, A., Haber-Pohlmeier, S., & Stapf, S. (2009). A fast field cycling nuclear magnetic
735 resonance relaxometry study of natural soils. *Vadose Zone Journal,* 8(3), 735-742.

736 Qin, H., Hu, T., Zhai, Y., Lu, N., & Aliyeva, J. (2020). The improved methods of heavy metals
737 removal by biosorbents: A review. *Environmental Pollution,* 258.

738 Rao, M. A., Di Rauso Simeone, G., Scelza, R., & Conte, P. (2017). Biochar based remediation
739 of water and soil contaminated by phenanthrene and pentachlorophenol. *Chemosphere,* 186, 193-
740 201.

741 Rao, M. M., Ramana, D. K., Seshaiah, K., Wang, M. C., & Chien, S. W. C. (2009). Removal of
742 some metal ions by activated carbon prepared from Phaseolus aureus hulls. *Journal of Hazardous*
743 *materials,* 166(2), 1006-1013.

744 Ravindiran, G., Ganapathy, G. P., Josephraj, J., & Alagumalai, A. (2019). A Critical Insight into
745 Biomass Derived Biosorbent for Bioremediation of Dyes. *ChemistrySelect,* 4(33), 9762-9775.

746 Rekharsky, M. V., & Inoue, Y. (1998). Complexation Thermodynamics of Cyclodextrins.
747 *Chemical Reviews,* 98(5), 1875-1918.

748 Rizzarelli, E., & Vecchio, G. (1999). Metal complexes of functionalized cyclodextrins as
749 enzyme models and chiral receptors. *Coordination Chemistry Reviews,* 188(1), 343-364.

750 Rubin Pedrazzo, A., Smarra, A., Caldera, F., Musso, G., Dhakar, N. K., Cecone, C., Hamedi, A.,
751 Corsi, I., Trotta, F. (2019). Eco-Friendly β-cyclodextrin and Linecaps Polymers for the Removal
752 of Heavy Metals. *Polymers,* 11(10), 1658.

753 Russo, M., Armetta, F., Riela, S., Chillura Martino, D., Meo, P. L., & Noto, R. (2015). Silver
754 nanoparticles stabilized by a polyaminocyclodextrin as catalysts for the reduction of nitroaromatic
755 compounds. *Journal of Molecular Catalysis A: Chemical,* 408, 250-261.

756 Russo, M., Spinella, A., Di Vincenzo, A., Lazzara, G., Correro, M. R., Shahgaldian, P., Lo Meo,
757 P., Caponetti, E. (2019). Synergistic Activity of Silver Nanoparticles and Polyaminocyclodextrins
758 in Nanosponge Architectures. *ChemistrySelect,* 4(3), 873-879.

759 Sarode, S., Upadhyay, P., Khosa, M. A., Mak, T., Shakir, A., Song, S., & Ullah, A. (2019).
760 Overview of wastewater treatment methods with special focus on biopolymer chitin-chitosan.
761 *International Journal of Biological Macromolecules,* 121, 1086-1100.

762 Sikder, M. T., Rahman, M. M., Jakariya, M., Hosokawa, T., Kurasaki, M., & Saito, T. (2019).
763 Remediation of water pollution with native cyclodextrins and modified cyclodextrins: A
764 comparative overview and perspectives. *Chemical Engineering Journal,* 355, 920-941.

765 Siyal, A. A., Shamsuddin, M. R., Low, A., & Rabat, N. E. (2020). A review on recent
766 developments in the adsorption of surfactants from wastewater. *Journal of Environmental*
767 *Management,* 254, 109797.

768 Stingaciu, L. R., Weihermüller, L., Haber-Pohlmeier, S., Stapf, S., Vereecken, H., & Pohlmeier,
769 A. (2010). Determination of pore size distribution and hydraulic properties using nuclear magnetic
770 resonance relaxometry: A comparative study of laboratory methods. *Water Resources Research,*
771 46(11).

772 Swaminathan, S., Vavia, P. R., Trotta, F., & Torne, S. (2007). Formulation of betacyclodextrin
773 based nanosponges of itraconazole. *Journal of inclusion phenomena and macrocyclic chemistry,*
774 57(1), 89-94.

775 Szejtli, J. (1998). Introduction and General Overview of Cyclodextrin Chemistry. *Chemical*
776 *Reviews,* 98(5), 1743-1754.

777 Tabushi, I., Kuroda, Y., & Mizutani, T. (1984). Functionalized cyclodextrins as artificial
778 receptors: Guest binding to bisimidazolyl-β-cyclodextrin-zinc. *Tetrahedron,* 40(3), 545-552.

779 Taka, A. L., Fosso-Kankeu, E., Pillay, K., & Mbianda, X. Y. (2018). Removal of cobalt and lead
780 ions from wastewater samples using an insoluble nanosponge biopolymer composite: adsorption
781 isotherm, kinetic, thermodynamic, and regeneration studies. *Environmental Science and Pollution*
782 *Research,* 25(22), 21752-21767.

783 Tong, M., & Yuan, S. (2012). Physiochemical technologies for HCB remediation and disposal:
784 A review. *Journal of Hazardous materials,* 229-230, 1-14.

785 Tran, H. N., You, S.-J., & Chao, H.-P. (2016). Thermodynamic parameters of cadmium
786 adsorption onto orange peel calculated from various methods: A comparison study. *Journal of*
787 *Environmental Chemical Engineering,* 4(3), 2671-2682.

788 Trotta, F. (2011). *Cyclodextrin Nanosponges and their Applications*. In *Cyclodextrins in*
789 *Pharmaceutics, Cosmetics, and Biomedicine* (pp. 323-342): John Wiley & Sons, Inc.

790 Trotta, F., Dianzani, C., Caldera, F., Mognetti, B., & Cavalli, R. (2014). The application of
791 nanosponges to cancer drug delivery. *Expert Opinion on Drug Delivery,* 11(6), 931-941.

792 Trotta, F., Shende, P., & Biasizzo, M. (2012). Method for preparing dextrin nanosponges.
793 Google Patents.

794 Trotta, F., Zanetti, M., & Cavalli, R. (2012). Cyclodextrin-based nanosponges as drug carriers.
795 *Beilstein Journal of Organic Chemistry,* 8, 2091-2099.

796 Vasconcelos, D. A., Kubota, T., Santos, D. C., Araujo, M. V. G., Teixeira, Z., & Gimenez, I. F.
797 (2016). Preparation of Aun quantum clusters with catalytic activity in β-cyclodextrin polyurethane
798 nanosponges. *Carbohydrate Polymers,* 136, 54-62.

799 Wang, J., & Wang, S. (2019). Preparation, modification and environmental application of
800 biochar: A review. *Journal of Cleaner Production,* 227, 1002-1022.

801 Wilson, L. D., Mohamed, M. H., & Berhaut, C. L. (2011). Sorption of aromatic compounds with
802 copolymer sorbent materials containing β-cyclodextrin. *Materials,* 4(9), 1528-1542.

803 Wilson, L. D., Mohamed, M. H., & Headley, J. V. (2011). Surface area and pore structure
804 properties of urethane-based copolymers containing β-cyclodextrin. *Journal of Colloid and*
805 *Interface Science,* 357(1), 215-222.

806 Wu, D., Hu, L., Wang, Y., Wei, Q., Yan, L., Yan, T., Li, Y., Du, B. (2018). EDTA modified β-
807 cyclodextrin/chitosan for rapid removal of Pb(II) and acid red from aqueous solution. *Journal of*
808 *Colloid and Interface Science,* 523, 56-64.

809 Yoshihisa, M., Toyoaki, K., & Yoshio, D. (1972). Complexes of Copper(II) with Cyclodextrins.
810 *Bulletin of the Chemical Society of Japan,* 45(10), 3229-3229.

811 Yuh-Shan, H. (2004). Citation review of Lagergren kinetic rate equation on adsorption reactions.
812 *Scientometrics,* 59(1), 171-177.

Zhang, Q., Hou, Q., Huang, G., & Fan, Q. (2020). Removal of heavy metals in aquatic environment by graphene oxide composites: a review. *Environmental Science and Pollution Research,* 27(1), 190-209.

Zhao, H.-t., Ma, S., Zheng, S.-y., Han, S.-w., Yao, F.-x., Wang, X.-z., Wang, S.-s., Feng, K. (2019). β–cyclodextrin functionalized biochars as novel sorbents for high-performance of Pb2+ removal. *Journal of Hazardous materials,* 362, 206-213.

Zheng, S., Xia, S., Han, S., Yao, F., Zhao, H., & Huang, M. (2019). β-Cyclodextrin-loaded minerals as novel sorbents for enhanced adsorption of Cd^{2+} and Pb^{2+} from aqueous solutions. *Science of the Total Environment,* 693, 133676.

Zhu, D. D., & Zhou, Q. X. (2018). A review on the removal of heavy metals from water using nanomaterials. *Journal of Agro-Environment Science,* 37(8), 1551-1564.

Graphical Abstract

Click here to access/download;Figure(s);TOC.jpg